Numerical Evaluation of the Two-Dimensional Generalized Exponential Integral

Martin Gimersky, *Student Member, IEEE*, Smain Amari, and Jens Bornemann, *Senior Member, IEEE*

***Abstract*— An exact technique for the evaluation of the two-dimensional generalized exponential integral—as required in structures involving rectangular planar radiators and transmission lines—is presented. It is shown that the singularity is integrable if integration is performed in polar coordinates. The integral can be calculated exactly and with minimal computational effort, even if integration over the origin of the coordinate system is required—regardless of whether the origin is an internal or boundary point of the integration region. Comparison with a standard technique proves the presented approach superior. Stability of the algorithm and convergence is discussed. Performance is demonstrated for the example of an asymmetrically edge-fed patch antenna.**

I. Introduction

Accurate calculation of the generalized exponential integral is of paramount importance for the method-of-moments solutions of problems involving radiating structures. Inaccuracies of the numerical evaluation of mutual and self-impedances can lead to grossly incorrect current distributions. In addition, varying the degree of inaccuracy of the numerically integrated elements of the impedance matrix is equivalent to tuning the results which, in effect, means inability to predict unknown values.

The generalized exponential integral in its one-dimensional form is well known from the calculation of mutual and self-impedances of wire antenna elements. The specific problem of calculating the self-impedance of a wire element of length $2x$ and radius a is, from the numerical point of view, reduced to the evaluation of the integral

$$I_1 = \int_{-x}^{x} \frac{e^{-jk\sqrt{x'^2+a^2}}}{\sqrt{x'^2+a^2}}\, dx'. \qquad (1)$$

The presence of radius a in the expression reflects sampling the electric field just above the surface of the wire, which is in direct correspondence with physical reality. Despite the fact that an infinitesimally thin wire ($a = 0$) is not of practical importance, it should not be left unnoticed that integral I_1 in (1) does not exist for $a = 0$.

A multitude of techniques for the evaluation of I_1 can be found in the literature, and we will mention only a few representatives here. In [1], the one-dimensional exponential integral is expressed in terms of three integrals where the first is available in closed form, while the remaining two are given by tabulated generalized sine and cosine integrals. In [2], I_1

Manuscript received May 9, 1995; revised April 30, 1996.
The authors are with the Laboratory for Lightwave Electronics, Microwaves and Communications (LLiMiC), Department of Electrical and Computer Engineering, University of Victoria, Victoria, BC, V8W 3P6, Canada.
Publisher Item Identifier S 0018-926X(96)07009-3.

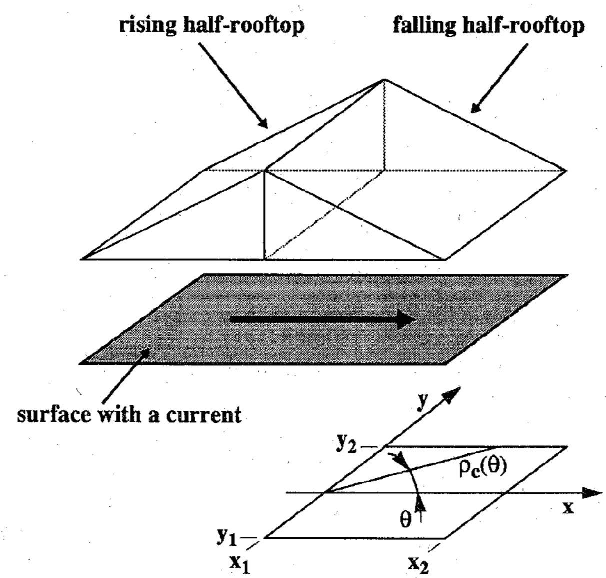

Fig. 1. A pair of rising and falling half rooftops representing a surface current, and the rectangular integration region of the falling half rooftop in the Cartesian coordinate system.

is expanded into a Maclaurin series, and an approximation accounts for only the first real and first imaginary terms. Of particular significance is the technique announced in [3] which is stable for a wire radius-to-wavelength ratio as small as 10^{-19} [3].

Planar radiators, by analogy, require evaluation of the two-dimensional integral

$$I_2 = \int_{x_1<0}^{x_2>0} \int_{y_1<0}^{y_2>0} \frac{e^{-jk\sqrt{x'^2+y'^2+a^2}}}{\sqrt{x'^2+y'^2+a^2}}\, dy'\, dx' \qquad (2)$$

which corresponds to the usage of pulses in the role of subsectional expansion functions in the method-of-moments formulation. If different expansion functions are desired, the integrand of I_2 needs to be properly modulated and the limits of integration may change, where the origin $(x', y') = (0, 0)$ may be located inside or on the boundary of the integration region. For example, in the rooftop-function representation, which employs pairs of rising and falling triangles as subsectional expansion functions (Fig. 1), e.g., [4], evaluation of

$$I_3 = \int_{0}^{x_2} \int_{-y_2}^{y_2} \left(1 - \frac{x'}{x_2}\right) \frac{e^{-jk\sqrt{x'^2+y'^2+a^2}}}{\sqrt{x'^2+y'^2+a^2}}\, dy'\, dx' \qquad (3)$$

is involved in the calculation of self-impedances related to falling half rooftops (modifications for a rising half rooftop are

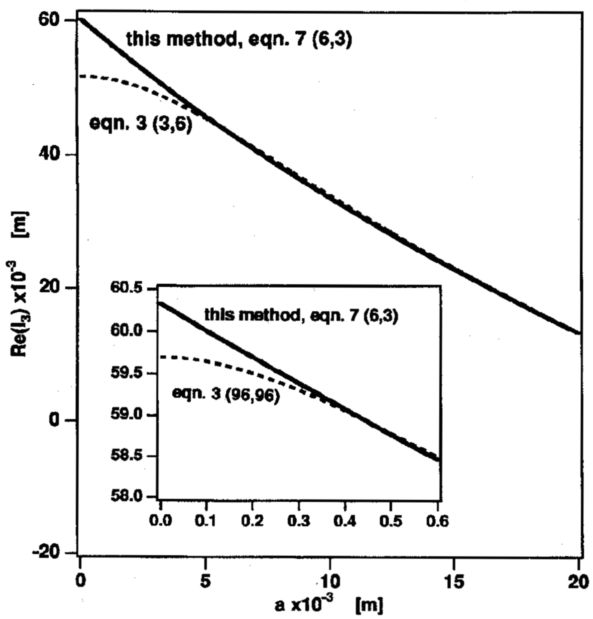

Fig. 2. Calculated values of the real part of integral I_3 versus a (parameters: $x_1 = 0$, $x_2 = 5$ cm, $y_1 = -3$ cm, $y_2 = 3$ cm, frequency = 2 GHz). Solid lines: six outer-/three inner-point Gaussian integration in polar coordinates according to (6); dashed line of principal figure: three outer-/six inner-point Gaussian integration in Cartesian coordinates according to (3); dashed line of inset: 96 outer-/96 inner-point Gaussian integration in Cartesian coordinates according to (3).

straightforward). It should be pointed out that while the case of $a = 0$ is of merely academic importance in one-dimensional wire antenna applications, it has a perfectly valid physical equivalent for two-dimensional planar radiator configurations; it corresponds to integrating the electric field on the surface of a radiating element.

Integrals of the types of I_2 and I_3 have been evaluated by techniques that, although different in approach to the problem, have one feature in common—they fail to integrate the singularity that emerges at $a = 0$ and $(x', y') = (0, 0)$. In addition, very often they implement various convenient approximations that reduce numerical complexity at the cost of introducing more inaccuracy and limiting the application range of the algorithm, often making it custom made for one particular class of problems or application.

In this paper, we show that the singularities of the two-dimensional generalized exponential integrals in (2), (3), which arise with $a = 0$, are integrable, that the integrals are finite, and that they can be stable and exactly calculated without any need for time-consuming computing.

II. Integral Calculation

The general configuration for integrals of the type of I_2 is depicted in Fig. 1. Instead of performing integration in the Cartesian coordinate system we evaluate I_2 in polar coordinates, resulting in

$$I_2 = \int_0^{2\pi} \int_0^{\rho_c(\theta)} \frac{e^{-jk\sqrt{\rho^2+a^2}}}{\sqrt{\rho^2 + a^2}} \rho \, d\rho d\theta \tag{4}$$

where $\rho = \sqrt{x'^2 + y'^2}$ and $\rho_c(\theta)$ is the radial distance from the origin of the coordinate system to the contour of the integration region. It is obvious that the technique is directly applicable also to the cases where the origin of the coordinate system is located outside of the integration region; in these cases the lower integration limit over ρ would be some positive value $\rho_{cl}(\theta)$ instead of zero. After the change of variables $u = \sqrt{\rho^2 + a^2}$ we get

$$I_2 = \frac{j}{k} \int_0^{2\pi} \left[e^{-jk\sqrt{\rho_c(\theta)^2+a^2}} - e^{-jk|a|}\right] d\theta. \tag{5}$$

Clearly, the singularity which arises at $a = 0$ in Cartesian coordinates [cf., (2)], has been removed, and the integral poses no numerical difficulties. Note that (5) is independent of the shape of the contour describing the boundary of the integration region. For the rectangular contour of Fig. 1, $\rho_c(\theta) = x_2/(\cos\theta)$ for the right vertical line, $\rho_c(\theta) = y_2/(\sin\theta)$ for the upper horizontal line, $\rho_c(\theta) = x_1/(\cos\theta)$ for the left vertical line, and $\rho_c(\theta) = y_1/(\sin\theta)$ for the lower horizontal line.

Finally, utilizing the result for I_2 and calculating the integral over ρ by parts, we evaluate I_3 as

$$I_3 = I_2 - \frac{j}{kx_2} \int_0^{2\pi} \cdot \left[\rho_c(\theta) e^{-jk\sqrt{\rho_c(\theta)^2+a^2}} - \int_0^{p_c(\theta)} e^{-jk\sqrt{\rho^2+a^2}} \, d\rho\right] \cdot \cos\theta \, d\theta. \tag{6}$$

Once again, the singularity is no longer present. Of course, the numerical integration over θ, although involved in both components of I_3, does not have to be performed in two separate cycles. This integration for two different integrands (where the second integrand requires also integration over ρ) can be executed in a single cycle; as a result of that, our software implementation of I_3 requires only two loops, one submerged in the other.

III. Numerical Results

Fig. 2 shows plots of the real part of integral I_3 versus a. Calculations produced by two different algorithms are presented: 1) two-dimensional Gaussian integration in Cartesian coordinates (dashed lines) and 2) the technique described in this paper, i.e., exact two-dimensional integration in polar coordinates, using the Gauss quadrature (solid lines). The Gaussian-integration results in polar coordinates (solid lines) were obtained by integrating in only three points in the inner integral and six points in the outer integral [cf., (6)], for each particular value of a. However, those in Cartesian coordinates (dashed lines) were calculated with six points in the inner and three points in the outer integral [cf., (3)]. This reversal of the number of points for inner and outer integrations in Cartesian coordinates produces more accurate results, because a higher number of points in the inner integral smooths the integrand of the outer integral. Each curve in Fig. 2 contains 2001 points and took 1.4 s of CPU time of an IBM RS/6000 530 machine.

Before evaluating the results of Fig. 2, some remarks about the presentation of values at $a = 0$ are in order. The solid

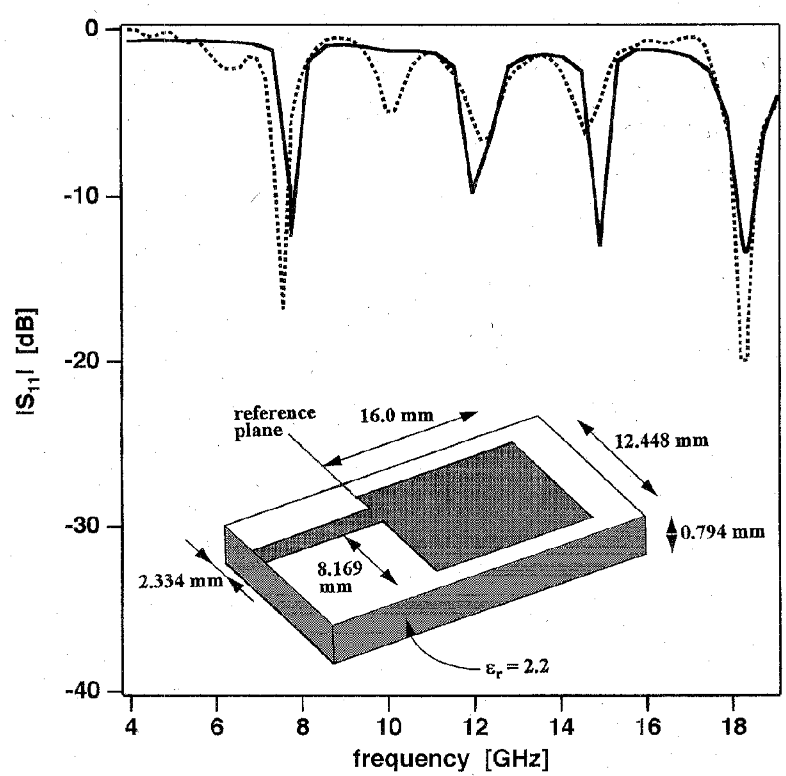

Fig. 3. An asymmetrically edge-fed rectangular patch, and frequency dependence of its input reflection coefficient. Dashed line: measurement of [5]. Solid line: our calculation involving the new integration procedure of this paper.

lines are calculated exactly at $a = 0$, as no singularity exists in (6). Also the dashed line is calculated at $a = 0$, but the numerical integration carefully avoids the sampling point $(x', y') = (0, 0)$, for which the integration in Cartesian coordinates (3) fails to produce a finite value.

As expected, the results of the Gaussian integration in Cartesian coordinates (dashed line) converge to those in polar coordinates (solid line) as a increases. Better convergence for smaller a can be achieved by significantly increasing the number of integration points in (3). This is demonstrated in the inset of Fig. 2, using 96×96 integration points in Cartesian coordinates. However, the CPU time increases from the aforementioned 1.4 s to 199.2 s which, clearly, makes a further increase of precision in Cartesian coordinates unreasonable. On the other hand, the new technique using integration in polar coordinates (6) is stable with respect to an increase in the number of integration points. The maximum difference between the (6, 3)- and (96, 96)-point integration in polar coordinates occurs at $a = 0$ and is 0.1% thus falls within the plotting accuracy of the solid line of the Fig. 2 inset.

No problems have been encountered when evaluating the imaginary part of I_3. Computations using integration in both Cartesian and polar coordinates are in good agreement.

Fig. 2 proves that both techniques are stable, but their accuracies are very different, especially for small values of a. While integrating in either polar or Cartesian coordinates proves that I_3 is *finite* and can be calculated exactly (even at $a = 0$), the convergence analysis of the Gaussian integration proves that our technique is superior to the integration in Cartesian coordinates. We have stressed out the precision of integration at $a = 0$ and at small a's, because these are the situations that are involved in the evaluation of self- and mutual impedances, respectively, of planar-radiator elements. Varying the degree of inaccuracy in the evaluation of the impedance elements results in a wide range of possible but inaccurate current distributions.

IV. Application

We have employed the new integration procedure of this paper to calculate the frequency dependence of the input reflection coefficient of an asymmetrically edge-fed rectangular patch depicted in the inset of Fig. 3. Our calculated values of $|S_{11}|$ (solid line) are plotted in comparison with measurement of [5] (dashed line). With the sole exception of the measured dip at 10.18 GHz, the calculation confirms the measurement over the entire frequency band. The slight ripple in the measurement in [5] is attributed to imperfections of measuring equipment. We have investigated the mechanism that gives rise to the dip of $|S_{11}|$ at 10.18 GHz and found that the dip is created by the feeding microstrip section and depends on its length. Because the length is not specified in [5], we subsequently varied the quantity and were able to move the dip over the entire frequency range; the solid line of Fig. 3 corresponds to the case in which the dip is below 4 GHz.

V. Conclusion

It is demonstrated that the two-dimensional generalized exponential integral, unlike the one-dimensional one, always exists and can be calculated exactly and without any need for extensive computing. Integration in polar coordinates over the radial variable ρ removes the singularity from the integrand and, therefore, leads to a stable and computationally efficient numerical algorithm. Only 6×3 points in the Gaussian quadrature are needed to achieve results accurate to better than 0.1%. Good agreement is observed between measured and calculated frequency dependences of the input reflection coefficient of an asymmetrically edge-fed rectangular patch antenna.

REFERENCES

[1] R. W. P. King, *The Theory of Linear Antennas.* Cambridge, MA: Harvard Univ. Press, 1956.
[2] R. F. Harrington, *Field Computation by Moment Method.* Malabar, FL: Krieger Publ., 1987, ch. 4, pp. 62–81.
[3] D. H. Werner, P. L. Werner, J. H. Huffman, A. J. Ferraro, and J. K. Breakall, "An exact solution of the generalized exponential integral and its application to moment method formulations," *IEEE Trans. Antennas Propagat.,* vol. 41, pp. 1716–1719, Dec. 1993.
[4] B. J. Rubin and S. Daijavad, "Radiation and scattering from structures involving finite-size dielectric regions," *IEEE Trans. Antennas Propagat.,* vol. 38, pp. 1863–1873, Nov. 1990.
[5] S. C. Wu, N. G. Alexopoulos, and O. Fordham, "Feeding structure contribution to radiation by patch antennas with rectangular boundaries," *IEEE Trans. Antennas Propagat.,* vol. 40, pp. 1245–1249, Oct. 1992.

Martin Gimersky (S'91) was born in Presov, Czechoslovakia, in 1965. He received the Engineer degree from the Faculty of Electrical Engineering, Czech Technical University, Pragu, Czechoslovakia, in 1988, and the Ph.D. degree in electrical engineering from the University of Victoria, Victoria, BC, Canada, in 1996.

From April to August 1996, he worked as a Post-Doctoral Fellow at the University of Manitoba, Winnipeg, MB, Canada. Since September 1996, he has been on the technical staff of Spar Aerospace, Ltd., Ste. Anne-de-Bellevue, PQ, Canada. His research interests are in microwave and millmeter-wave antennas and numerical modeling in electromagnetics.

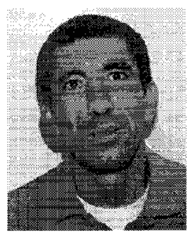

Smain Amari received the E.S. degree in physics and electronics from Constantine University, Algeria, in 1985, and the M.S. (electrical engineering) and Ph.D. degrees (physics) from Washington University, St. Louis, MO, in 1989 and 1994, respectively.

His main interests are in numerical methods in electromagnetics, numerical analysis, applied mathematics, applied physics, and application of quantum field theory in quantum many-particle systems.

Jens Bornemann (M'87–SM'90) was born in Hamburg, Germany, on May 26, 1952. He received the Dipl.-Ing. and the Dr.-Ing. degrees, both in electrical engineering, from the University of Bremen, Germany, in 1980 and 1984, respectively.

From 1980–1983, he was a Research and Teaching Assistant in the Microwave Department at the University of Bremen, Germany, where he worked on quasi-planar waveguide configurations and computer-aided E-plane filter design. In 1985, after a two-year period as a Consulting Engineer, he again joined the University of Bremen, and was employed as an Assistant Professor. Since April 1988, he has been with the University of Victoria, Victoria, B.C., Canada, where he is currently a Professor in the Department of Electrical and Computer Engineering. He is a co-author of *Waveguide Components for Antenna Feed Systems—Theory and Design* (Norwood, MA: Artech House, 1993) and has authored or co-authored more than 100 technical papers. He also serves on the editorial board of the IEEE TRANSACTIONS ON MICROWAVE THEORY AND TECHNIQUES and the *International Journal of Numerical Modelling*. His research activities include microwave/millimeter-wave components and systems design, and problems of electromagnetic field theory in integrated circuits and radiating structures.

Dr. Bornemann is a Registered Professional Engineer in the Province of British Columbia, Canada, and was a Fellow of the British Columbia Advanced Systems Institute from 1992 to 1995. He was one of the recipients of the A.F. Bulgin Premium of the Institution of Electronic and Radio Engineers in 1983.